Neuropharmacology 63 (2012) 784–797

Contents lists available at SciVerse ScienceDirect

Neuropharmacology

journal homepage: www.elsevier.com/locate/neuropharm

Presynaptic α_2-adrenoceptors control the inhibitory action of presynaptic CB_1 cannabinoid receptors on prefrontocortical norepinephrine release in the rat

Hardy Richter [a,b], Filipe M. Teixeira [c], Samira G. Ferreira [c], Ágnes Kittel [a], Attila Köfalvi [c], Beáta Sperlágh [a,b,*]

[a] Laboratory of Molecular Pharmacology, Institute of Experimental Medicine, Hungarian Academy of Sciences (IEM-HAS), H-1083 Budapest, Szigony u. 43, Hungary
[b] Department of Pharmacology and Pharmacotherapy, Semmelweis University, Budapest, Hungary
[c] Laboratory of Neuromodulation and Metabolism, Center for Neurosciences and Cell Biology of Coimbra, 3004-504 Coimbra, Portugal

ARTICLE INFO

Article history:
Received 17 November 2011
Received in revised form
15 May 2012
Accepted 5 June 2012

Keywords:
α_{2A} adrenergic receptor
CB_1 receptor
Norepinephrine
Release
Prefrontal cortex

ABSTRACT

Endocannabinoids play a crucial neuromodulator role in both physiological and pathological states in various brain regions including the prefrontal cortex (PFC). We examined, whether presynaptic cannabinoid receptors are involved in the modulation of basal and electrical field stimulation-evoked [^{3}H] norepinephrine ([^{3}H]NE) release from rat PFC slices. WIN55,212-2, a nonselective CB_1 receptor (CB_1R) agonist, inhibited the electrical stimulation-evoked efflux of [^{3}H]NE in a concentration-dependent fashion, which was antagonized by the CB_1R antagonist/inverse agonist, AM251 (1 μM). Idazoxan, a selective α_2-adrenoceptor antagonist, augmented the evoked [^{3}H]NE release. In the presence of idazoxan, the effect of WIN55,212-2 was exacerbated or attenuated, depending on the applied concentration and stimulation frequency. Moreover their combined, but not individual application elicited a depressive-like phenomenon in the forced-swim test. These data were bolstered with fluorescent and confocal microscopy analysis, which revealed that CB_1R immunoreactivity co-localized with dopamine-β-hydroxylase positive (i.e. noradrenergic) fibers and the inhibitory α_{2A} adrenergic autoreceptors ($\alpha_{2A}R$) in the PFC. Furthermore, idazoxan triggered a decrease in CB_1R density in the PFC, suggesting that high extracellular level of norepinephrine downregulates CB_1Rs.

1. Introduction

The PFC circuit exerts the cognitive control over complex behavior and is also an integral part of the reward system. Therefore, its modulation has multiple implications in a number of neuropsychiatric disorders. These include schizophrenia, attention deficit hyperactivity disorder (ADHD), aggressive personality disorder, Parkinson's disease and other more frequent health burdens including depression, addiction and eating disorders. Many of those are characterized by an increased norepinephrine turnover in this brain region (Arnsten, 2011; Gamo and Arnsten, 2011; Ramos and Arnsten, 2007) and agents that enhance monoaminergic activity in the prefrontal cortex are effective therapeutic options in treating these disorders (Bymaster et al., 2002a, b; Westerink et al., 2001; Zhang et al., 2000). Altered signaling in the PFC has been associated with the executive dysfunction component of addiction with its core deficits represented by loss of control, impulsivity and impaired decision making (Koob and Volkow, 2010). In fact, stress experienced during food- or drug-restriction leads to increased NE release from varicosities of *locus coeruleus* noradrenergic neurons in the PFC through activation of the hypothalamo-pituitary axis (HPA) and thereby contributes to the transition from reward to addiction (Koob and Kreek, 2007). The PFC and its α_{2A} adrenoceptors ($\alpha_{2A}R$) are also instrumental for spatial working memory (Arnsten et al., 1988; Wang et al., 2007) as well as emotional behavior (Zhang et al., 2009).

It is known that consumption of cannabis, especially during periods of brain development, can precipitate mental illness – in particular PFC disorders – in genetically susceptible people (Malone et al., 2010; Bossong and Niesink, 2010). Moreover, as revealed by the STRADIVARIUS trial, the inhibition of CB_1 receptors (CB_1R) can also lead to an increased incidence of depression and suicide (Nissen et al., 2008).

The finding that cannabis use impairs the ability to effectively focus attention and reject irrelevant information suggests an impact of cannabinoids on the noradrenergic coeruleo-cortical pathway. Noradrenergic neuromodulation is necessary for

* Corresponding author. Laboratory of Molecular Pharmacology, Institute of Experimental Medicine, Hungarian Academy of Sciences, H-1450 Budapest, POB 67, Hungary. Tel.: +36 1 210 9970; fax: +36 1 210 9423.
E-mail address: sperlagh@koki.hu (B. Sperlágh).

0028-3908/$ – see front matter © 2012 Elsevier Ltd. All rights reserved.
http://dx.doi.org/10.1016/j.neuropharm.2012.06.003

motivational salience attribution to reward-related stimuli through dopaminergic signaling in the *nucleus accumbens* (nAcc), thereby mediating hedonic impact of reward or aspects of reward learning (Koob and Volkow, 2010). The impaired response of the prefrontal-accumbal catecholamine system to highly motivating stimuli in the addicted state could be explained by this phenomenon.

Despite the abundance of data on the action of cannabinoids on complex behavioral changes mediated by the monoaminergic system, relatively few investigations concentrated on the interaction of cannabinoids and norepinephrine on the cellular level. Neuroanatomical data suggest that dopamine-β-hydroxylase-(DβH) positive varicose axon terminals of the PFC express CB_1R immunoreactivity (Oropeza et al., 2007), although the majority of CB_1Rs are localized to GABAergic and glutamatergic nerve terminals in cortical areas (Bodor et al., 2005; Lafourcade et al., 2007; Ferreira et al., in press). However, previous functional data on the modulation of NE release in the PFC are conflicting: *in vivo* both cannabinoid agonists and antagonists increase the efflux of NE from prefrontal cortex (Oropeza et al., 2005; Page et al., 2008; Tzavara et al., 2003), whilst in other regions of the brain such as the hippocampus the direct effect of activation of CB_1Rs on NE release is inhibition (Kathmann et al., 1999; Schlicker et al., 1997).

In contrast, it is well established that central noradrenergic nerve terminals are equipped with presynaptic $\alpha_{2A}Rs$, another G protein-coupled receptor (GPCR) the activation of which inhibits the release of NE (Starke, 2001). Moreover, these receptors are also activated by NE released upon neuronal activity – thereby executing an important fine-tuning mechanism, i.e. the auto-inhibition of transmitter release. In the primate PFC, α_2-adrenoceptors predominantly belonging to the α_{2A-D} subtype are immunolocalized to both pre- and post-synaptic sites, and presynaptic $\alpha_{2A}Rs$ are also expressed by DβH positive varicosities (Aoki et al., 1998; Wang et al., 2007). As both CB_1R and $\alpha_{2A}Rs$ utilize $G_{i/o}$ downstream signaling cascades, the possibility arises that there might be interplay between them. The activation of $\alpha_{2A}Rs$ improves regulation of attention, behavioral inhibition and task planning in humans, whereas NE depletion has been shown to increase distractibility during neuropsychological testing.

Here we report for the first time that CB_1Rs inhibit electrical field stimulation-evoked [^{3}H]norepinephrine ([^{3}H]NE) release from rat PFC slices. In addition, we reveal a dual interaction between the cannabinoid mediated suppression of NE efflux and its endogenous autoinhibition by $\alpha_{2A}Rs$. In fact, relief from $\alpha_{2A}R$ autoinhibition by idazoxan either facilitated or attenuated cannabinergic neuromodulation, depending on the concentration of agonist and the applied stimulation frequency, which may indicate changes in fine modulation of involved signaling pathways.

2. Materials and methods

2.1. Animals

All studies were conducted in accordance with the principles and procedures outlined in European Communities Council Directive of 24 November 1986 (86/609/EEC) and by FELASA and were approved by the Institutional Animal Care and Use Committee of the Hungarian Academy of Sciences. All efforts were done to minimize the suffering of the animals and the number of animals used.

Animals were housed in a SPF facility, with 12 h light on/off cycles and *ad libitum* access to food and water. Male Wistar rats (140–200 g, 8–10-week old) were bred in the local animal house (IEM HAS, Budapest Hungary) or purchased from Charles-River (Barcelona, Spain). CB_1R null-mutant (knockout) male mice (Ledent et al., 1999) and their wild-type littermates on CD-1 background, genotyped from the tail, were housed as detailed above until being sacrificed.

2.2. [^{3}H]NE release experiments

[^{3}H]NE release experiments were performed according to a method similar to the one described by Csölle et al. (2008). Young adult male Wistar rats weighing 120–150 g were selected, as the time-course of changes in synaptic density of CB_1 receptors in the first 6 months of age are minimal, i.e. less than 10 percent, as shown by Canas et al. (2009). Briefly, animals were anesthetized by brief CO_2 inhalation and decapitated. 400 μm coronal brain slices containing the frontal associative cortex (Paxinos and Watson, Rat Brain Atlas, 1998) were prepared with a McIlwain tissue chopper and loaded with [^{3}H]NE (10 μCi/ml, Amersham International Plc, UK, specific activity: 39 Ci/mmol) for 45 min at 37 °C in Krebs' solution and gassed with 95% O_2 and 5% CO_2. The perfusion solution was supplemented with Na_2EDTA (0.03 mM) and ascorbic acid (0.3 mM). Tissue slices were then superfused with Krebs' solution at 37 °C at a rate of 0.65 ml/min. After the pre-perfusion period (60 min), 3 min samples of the effluent were collected and assayed for radioactivity. Electrical field stimulations (EFS1, EFS2) were delivered by a Grass S88 stimulator, during the 3rd and 13th sample of the collection period using the following parameters: 25 V, 1 ms, 240 pulses at 2 Hz, 10 Hz, or 100 Hz, respectively. Unless otherwise stated, drugs were applied to the perfusion fluid 18 min before EFS2. At the end of each experiment, tissues were homogenized in 0.5 ml 10% trichloroacetic acid. A 0.5 ml aliquot of the superfusate and 0.1 ml of the tissue supernatant were added to 2 ml of scintillation cocktail (Ultima Gold, Packard). The liberated tritium was measured with a Packard 1900 TR liquid scintillation counter and expressed as the percentage of the amount of radioactivity in the tissue at the sample collection time (fractional release, %). The net release evoked by EFS (FRS1, FRS2) was calculated by the area-under-the-curve (AUC) method, i.e. subtracting the resting release calculated from the pre-stimulation period from the release measured during and after EFS. The effects of the drugs on EFS-evoked release of [^{3}H]NE were expressed as FRS2 over FRS1 (FRS2/FRS1) ratios. When concentration–response curves were generated, these values were expressed as percentage of respective control FRS2/FRS1 ratios, measured in the absence of drugs. To calculate the resting efflux, the mean of the tritium content of the samples collected immediately before the respective stimulation was taken into account. The tissue tritium uptake was determined as the total release plus the tissue content after the experiment and expressed in Bq/g, which reflects the content of radioactivity of the slices after the 60 min washout period, i.e. the radioactivity that is specifically taken up by the tissue. Previous high-performance liquid chromatography (HPLC) analyses using similar protocols showed that the majority of tritium efflux released by electrical field stimulation represents [^{3}H]NA.

2.3. Behavior experiments

2.3.1. Forced swim test

Male Wistar rats (250–300 g) were kept for 1 week before behavior tests in the experimental room. All experiments and treatments were carried out during the light phase (7.00 AM–7.00 PM). Each rat was placed in a transparent glass cylinder filled with water (22 ± 0.5 °C) and submitted to a single 6-min of forced swim test period. Fresh water was used for each rat, and four animals were tested simultaneously. WIN55,212-2 (0.2 mg/kg), idazoxan (0.5 mg/kg i.p.) or their combination were injected i.p. 30 min before test. The doses were chosen based on literature data (Bambico et al., 2007; Zhang et al., 2009). After the test period, animals were removed from the cylinder, dried with paper towels, and a clean towel was left in the home-cage for an hour to avoid cooling. Behavior was video-recorded during the experiments and analyzed later with a computer-based event recorder by an experimenter blind to the treatment. Immobility was defined as floating, that is when the animals were motionless or made only small movements to keep their head above water. The duration of immobility was expressed as a percentage of the total test period.

2.3.2. Open field test

Experiments were performed in the light phase under dimmed lights (~16 lux). Each animal was placed in the center of a nontransparent plexiglas arena (dimensions: 40 × 40 × 40 cm) for a habituation period of 30 min and then locomotor activity of the animals was recorded for 90 min using a video camera positioned above the arena. To measure locomotor activity video files were analyzed offline by converting them into single frames (25 frames/second) and a custom-written motion tracking algorithm was applied within the image processing software ImageJ. The total distance in meters was expressed in cm for the 90 min of the experiment.

2.4. Microscopy sections

Under deep sodium pentobarbital anesthesia (100 mg/kg body weight, i.p.), male Wistar rats and CB_1R null-mutant mice of the CD-1 strain and their wild-type littermates were fixed transcardially with a fixative (4% paraformaldehyde in 0.1 M phosphate buffer (PB), pH 7.4). Their brains were removed and immersed in fixative overnight and then kept in 30% sucrose in physiological saline (0.9% NaCl) for at least 48 h before sectioning. 40-μm-thick sections from the mouse brains and 30-μm-thick sections from the rat brains were cut using a cryostate microtome (Leica Microsystems, Milton Keynes, UK) and collected into 0.1 M PBS containing 0.1% sodium azide.

2.5. Immunohistochemistry

Experiments were carried out as described before (Ferreira et al., in press). Free floating sections were blocked in 10% normal goat serum (Vector Laboratories,

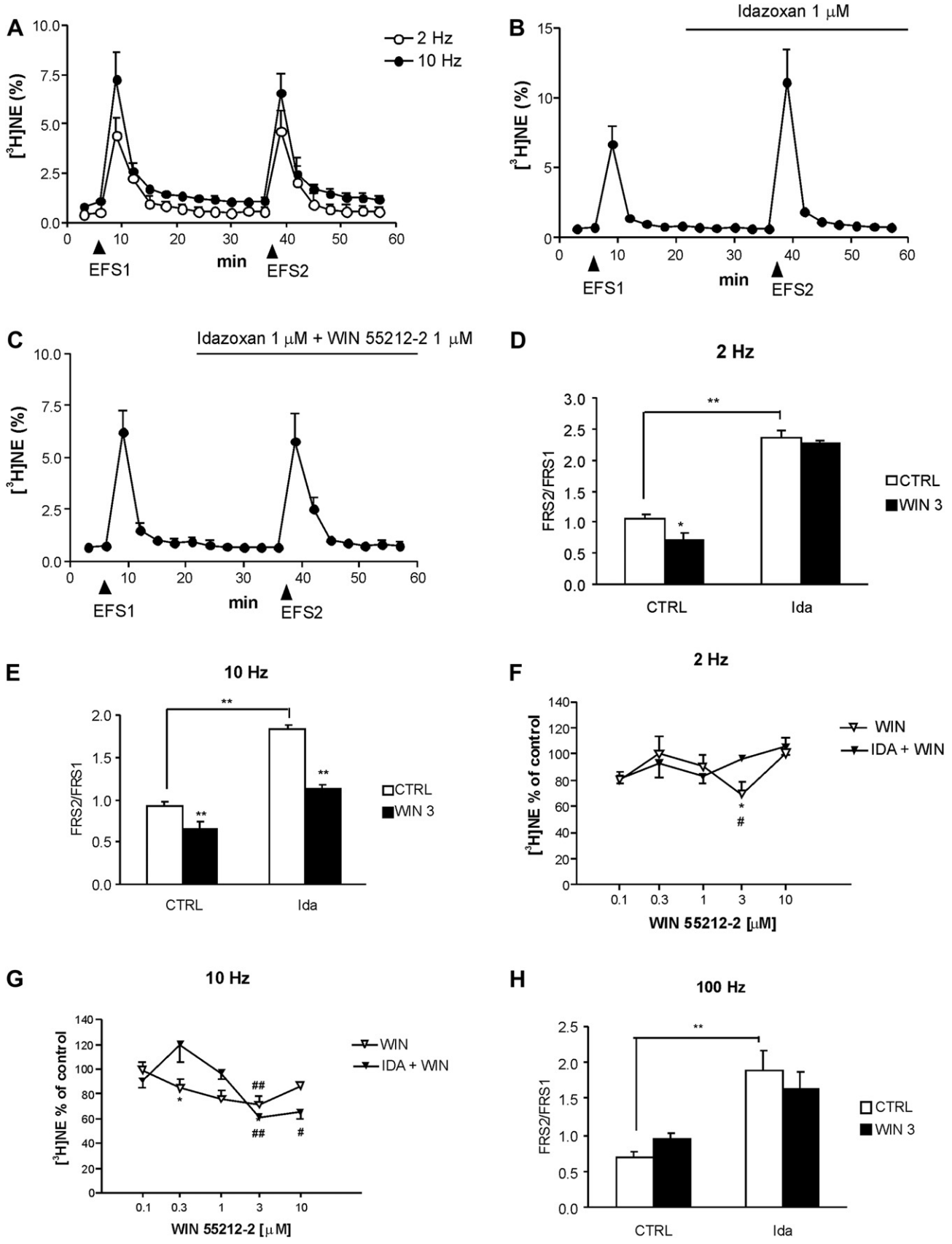

Fig. 1. A: Basal and electric field stimulation-evoked [^{3}H]NE release at 2 Hz and 10 Hz stimulation frequencies in the absence of drugs. The stimulation periods EFS1 and EFS2 are indicated with arrowheads. Data are expressed as fractional release (%, for calculation, see Materials and methods). B: Antagonism of α_{2A}Rs by idazoxan (1 μM) markedly enhances [^{3}H]NE overflow from PFC preparations. EFS was used at 10 Hz (arrows, EFS1, EFS2), idazoxan was applied as indicated by the horizontal bar. Data are expressed as fractional release

CA, USA)/5% BSA/0.3% Triton X-100 for 40 min and incubated overnight in a primary antibody cocktail of guinea pig anti-CB_1R (1:2000; Frontier Science, Hokkaido, Japan; see (Fukudome et al., 2004; Uchigashima et al., 2007) and/or mouse anti-dopamine-β-hydroxylase (DβH; 1:100; Abcam, UK) and/or rabbit anti-$\alpha_{2A}R$; 1:100; Abcam, UK). Sections were then washed in phosphate buffer (PB; 0.1 M) and incubated with a secondary antibody cocktail of DyLight 405, 488, and 594 goat anti-guinea-pig, anti-rabbit as well as anti-mouse (all at 1:200; Kirkegaard & Perry Laboratories, Inc, USA), for 2 h. After washing in PB 0.1 M, the sections were mounted on polylysine-coated slides, coverslipped using degassed Fluorescence Mounting Medium (Dako, Denmark) and then left to dry overnight at 4 °C. Low magnification images were taken on a Zeiss Axiovert 200 microscope equipped with AxioVision software and MosaiX module. Confocal images were taken using a Zeiss LSM510 META confocal microscope. While the CB_1R staining was essentially similar to previous data (e.g. Bodor et al., 2005) in the rat and wild-type (WT) mouse brain, no immunostaining was detected in the CB_1R knockout mouse brain sections at any resolution (Fig. 3G) or with the secondary antibodies in the absence of the primary antibodies (Figure not shown).

2.6. Immunohistochemical experiments on sections prepared from acute brain slices

Male Wistar rats were decapitated, 400 μm coronal brain slices containing the frontal associative cortex were prepared as described above and immediately put in Krebs' solution and then transferred into four polypropylene tissue chambers. Under continuous perfusion with aerated Krebs solution at a rate of 0.65 ml/min, electric field stimulations (EFS1, EFS2) using a Grass S88 Stimulator were applied 9 and 39 min after beginning of the perfusion with the following parameters: 25 V, 10 Hz, 1 ms, 240 pulses. Drugs (none, 1 μM idazoxan or 3 μM xylazine, respectively) were applied into the perfusion solution 18 min before EFS2. After 60 min, samples were transferred into 4% paraformaldehyde in 0.1 M phosphate-buffered saline fixative solution for an hour at room temperature. After thorough washing in PBS, 35 μm sections were cut using a vibrating microtome (VT1000S; Leica Microsystems, Milton Keynes, UK). Sections were then transferred to 30% sucrose in PB at 4 °C until they sank. Freeze-thawing in liquid nitrogen was applied to increase the penetration of antisera used for immunostaining. Subsequently, all washing steps and dilutions of the antibodies were done in 0.05 M TBS, pH 7.4. After extensive washing in TBS, the sections were blocked in the mixture of 3% donkey and 3% normal horse serum (Jackson ImmunoResearch Europe Ltd. Newmarket, Suffolk, UK) for 2 h, and then incubated with the above mentioned affinity-purified guinea-pig anti-CB_1R antibody (1 μg/ml) for a minimum of 48 h at 4 °C. Following extensive washing steps, DyLight 488 AffiniPure Donkey Anti-Guinea pig IgG (Jackson ImmunoResearch) were applied in dilution 1:400 overnight. Sections incubated without primary antibodies served as controls. After the final washes sections were transferred onto microscopic slides and mounted in Vectashield (Vector Laboratories; Burlingame, CA, USA). Confocal images were acquired at the same depth of the sections (10 μm) at same acquisition parameters with a Nikon A1R confocal system on an inverted Nikon Ti-E microscope (objective 20X DIC N1, numerical aperture 0.45) equipped with NIS-Elements C software. Images were edited, and brightness as well as contrast were adjusted, if necessary, using Adobe Photoshop CS3 (San Jose, CA, USA). Densitometric analyses were performed by the ImageJ software.

2.7. Materials

The following materials were used: [^{3}H]norepinephrine, (R)-(+)-[2,3-dihydro-5-methyl-3-(4-morpholinylmethyl)pyrrolo[1,2,3-de]-1,4-benzoxazin-6-yl]-1-naphthalenylmethanone mesylate (WIN55,212-2), N-(piperidin-1-yl)-5-(4-iodophenyl)-1-(2,4-dichlorophenyl)-4-methyl-1H-pyrazole-3-carboxamide (AM251), (5Z,8Z,11Z,14Z)-N-(4-hydroxy-2-methylphenyl)-5,8,11,14-eicosatetraenamide (VDM11), 2-(1,4-Benzodioxan-2-yl)-2-imidazoline hydrochloride (idazoxan) (all from Tocris Bioscience, Bristol, UK), D-amphetamine, okadaic acid, xylazine (Sigma, St. Louis, MO, USA). AM251 was dissolved in dimethyl sulfoxide (DMSO), WIN55,212-2 was dissolved in 0.1 M HCl and VDM11 was dissolved in TocrisolveTM100. The maximal concentrations of vehicles used had no significant effect on the release of [^{3}H]NE. In behavior experiments WIN55,212-2 was dissolved in Tween80 and further diluted in saline.

The composition of the Krebs' solution was the following (in mM): NaCl 113, KCl 4.7, $CaCl_2$ 2.5, KH_2PO_4 1.2, $MgSO_4$ 1.2, $NaHCO_3$ 25, and glucose 11.5. All solutions were prepared on the day of use.

2.8. Statistics

All data are expressed as means ± S.E.M. of n observations. The statistical analyses were made by Student's t-test (pair-wise comparisons), or one-way ANOVA followed by the Tukey test (multiple comparisons). Concentration–response curves were generated by the GraphPad Prism 5.04 software and analyzed by 2-way-ANOVA, followed by a Fisher-LSD post-hoc test. P values of less than 0.05 were considered statistically significant.

3. Results

3.1. [^{3}H]NE release experiments

After the PFC slices were loaded with [^{3}H]NE, the average tissue uptake of radioactivity was $1.067 \pm 0.16 \times 10^5$ Bq/g ($n = 6$, for calculation see Materials and methods). After 60 min pre-perfusion the average basal release in a 3-min fraction was 0.51 ± 0.12% ($n = 6$) of the total actual tissue tritium content and remained fairly constant until the end of the sample collection. To induce Ca^{2+}-dependent vesicular release and different noradrenergic autoreceptor occupancy, we evoked the efflux of [^{3}H]NE with low (2 Hz), medium (10 Hz) and high (100 Hz) frequency electrical field stimulation (EFS). Low frequency EFS (25 V, 2 Hz, 1 ms, 240 pulses) elicited a rapid and transient increase in the basal [^{3}H]NE efflux: the total tritium release evoked by stimulation was 7.04 ± 1.6% ($n = 6$, Fig. 1A). The second stimulation (EFS2) elicited a similar amount of tritium release, resulting in an FRS2/FRS1 ratio of 1.057 ± 0.07 ($n = 6$, Fig. 1A). When the stimulation frequency was elevated to 10 Hz, without altering other parameters, the stimulation-evoked release was 7.85 ± 1.08% (Fig. 1A, $n = 6$, $P > 0.05$ vs. 2 Hz, Fig. 1A). When high frequency (100 Hz) stimulation was applied, a decline in the amount of stimulation-evoked release was observed (4.53 ± 0.37%, $n = 8$, $P < 0.05$ vs. 10 Hz). Nevertheless, the evoked release of tritium remained fairly reproducible under these conditions (10 Hz, FRS2/FRS1: 0.93 ± 0.04, $n = 6$; 100 Hz, FRS2/FRS1: 0.71 ± 0.05, $n = 8$).

(%). C: The inhibitory effect of WIN55,212-2 (1 μM) measured in the presence of idazoxan (1 μM). EFS was applied at 10 Hz (arrows, EFS1, EFS2), drugs were applied as indicated by the horizontal bar. Data are expressed as fractional release (%) D: The inhibitory action of WIN55,212-2 (3 μM, WIN 3) on stimulation-evoked [^{3}H]NE release at 2 Hz EFS is attenuated when α_{2A}Rs are antagonized using idazoxan (1 μM, Ida) simultaneously, as shown by FRS2/FRS1 ratios in the absence (CTRL) and presence of WIN55,212-2 (WIN 3). CTRL: control. Asterisks indicate significant differences from respective controls or between control and idazoxan treated slices, calculated by the Student's t test (*$P < 0.05$, **$P < 0.01$). E. At 10 Hz EFS, WIN55,212-2 (3 μM) significantly suppressed [^{3}H]NE release, both in the absence (CTRL) and presence of idazoxan (Ida; 1 μM). Data are expressed as FRS2/FRS1 ratios, measured in the absence (CTRL) and presence of WIN55,212-2 (WIN 3). Asterisks indicate significant differences from respective controls or between control and idazoxan treated slices, calculated by the Student's t test (**$P < 0.01$). F: Concentration-dependent inhibitory effect of WIN55,212-2 in the presence (IDA + WIN) and absence (WIN) of idazoxan (1 μM) at 2 Hz EFS. Note that WIN55,212-2 alone achieved maximal inhibitory effect on [^{3}H]NE efflux at 3 μM ($^{\#}P < 0.05$, compared to drug-free control), whereas in the presence of idazoxan only slight, insignificant inhibition was observed at concentrations of 1 μM and below. Moreover, Fisher LSD post-hoc test following 2-way-ANOVA revealed a significant difference between the absence and presence of idazoxan, when 3 μM of WIN55,212-2 was used (*$P < 0.05$). Experiments were performed according to the protocol shown on A–C, but note that the results here are expressed as percentage of respective control FRS2/FRS1 ratios measured in the presence (IDA) and absence (CTRL) of idazoxan. G: Concentration-dependent inhibitory effect of WIN55,212-2 in the presence (IDA + WIN) and absence (WIN) of idazoxan (1 μM) at 10 Hz EFS. Results are expressed as percentage of respective control FRS2/FRS ratios measured in the presence (IDA) and absence (CTRL) of idazoxan. Experiments were performed according to the protocol shown on A–C. 2-way ANOVA revealed a significant WIN treatment ($F_{WIN}(1,66) = 6.461$, $P = 0.000061$) and interaction effect between WIN55,212-2 and idazoxan ($F_{interaction}(1,66) = 3.351$, $P = 0.0092$). Asterisks show significant differences from respective controls ($^{\#}P < 0.05$, $^{\#\#}P < 0.01$) and between the presence and absence of idazoxan (*$P < 0.05$) as indicated by Fisher LSD post-hoc test following 2-way ANOVA. Note that the inhibitory effect of WIN55,212-2 was exacerbated in the presence of idazoxan (1 μM) in concentrations above 3 μM i.e. the effect of WIN55,212-2 was significant in the presence of idazoxan only. In contrast, the inhibitory effect exerted by 0.3 μM WIN55,212-2 was significantly attenuated by the co-application of idazoxan (1 μM). H: At 100 Hz EFS, idazoxan (1 μM) similarly augmented [^{3}H]NE release as in the experiments at lower stimulation frequencies. WIN55,212-2 did not affect [^{3}H]NE efflux either in the absence or presence of idazoxan (1 μM). Data are expressed as FRS2/FRS1 ratios, measured in the absence (CTRL) and presence of WIN55,212-2 (WIN 3). Asterisks indicate significant differences from respective controls or between control and idazoxan treated slices, calculated by the Student's t test (**$P < 0.01$). Data represent the mean ± S.E.M. of 4–12 identical experiments.

To test the involvement of the axon potential propagation in the [^{3}H]NE efflux evoked by electrical stimulation, the effect of tetrodotoxin (TTX) was examined. Inhibition of the voltage-dependent Na^+ channels by TTX (3 μM) almost totally inhibited the stimulation-evoked release (FRS2/FRS1 = 0.05 ± 0.01, n = 6; $P < 0.005$ vs. control) at 10 Hz. This finding indicates that NE released in response to field stimulation is associated with ongoing neuronal activity. When the slices were superfused with Ca^{2+}-free Krebs' solution supplemented with EGTA (1 mM), the evoked release of [^{3}H]NE was inhibited by more than 97% (FRS1 = 0.168 ± 0.06%, n = 6; $P < 0.001$ vs. control) without affecting the basal efflux (1.07 ± 0.15%, n = 6, and 1.34 ± 0.33%, n = 6, in the presence and absence of $[Ca^{2+}]_o$, respectively, $P > 0.05$). The majority of the evoked release could therefore be regarded as Ca^{2+}-dependent release.

Idazoxan (1 μM), a selective α_{2A}R antagonist, whilst having no effect on basal efflux (0.65 ± 0.034% and 0.75 ± 0.05% in the presence and absence of idazoxan, n = 6, $P > 0.05$), significantly increased stimulation-evoked release of [^{3}H]NE (Fig. 1B, D, E, H) at any of the frequencies tested, showing that α_{2A}R-mediated autoinhibition of NE release operates under these conditions. The maximal increase in release evoked by idazoxan was 97.71 ± 4.73% at 10 Hz, obtained at the concentration of 1 μM (Fig. 1B, E). Increasing its concentration to 3 μM elicited no further augmentation of the [^{3}H]NE efflux (data not shown).

In the following set of experiments the effect of the non-selective synthetic cannabinoid agonist WIN55,212-2 was examined on the electrical field stimulation-evoked release of [^{3}H]NE at different stimulation frequencies. WIN55,212-2 was without significant effect on basal [^{3}H]NE efflux at 1 μM (0.42 ± 0.02% and 0.50 ± 0.04% in the presence and absence of WIN55,212-2, n = 6, $P > 0.05$) and in any other concentrations tested (data not shown).

The effect of WIN55,212-2 on stimulation-evoked [^{3}H]NE efflux was at first examined at 2 Hz stimulation frequency, and a significant inhibitory effect was observed in 3 μM concentration, which was abolished in the presence of idazoxan (1 μM) (Fig. 1D). This finding indicated that there is an interaction between α_{2A}Rs and CB_1Rs, both present on presynaptic nerve terminals. Then, the effect of WIN55,212-2 was tested in different concentrations in the absence and presence of idazoxan, and the data were expressed as percentage of respective controls. Two-way ANOVA analysis revealed a slight, but significant effect of WIN55,212-2 treatment (Fig. 1F, F_{WIN} (1,61) = 2.447, P = 0.043), but there was no significant interaction between WIN55,212-2 and idazoxan (Fig. 1F, $F_{interaction}$ (1,61) = 0.998, P = 0.426). However, when post hoc comparisons were run, the effect of WIN55,212-2 at 3 μM measured in the presence of idazoxan was significantly different from the values measured in the absence of the α_{2A}R antagonist (Fig. 1F, 68.87 ± 9.82%, and 96.54 ± 2.11% of control in the absence and presence of idazoxan, respectively, n = 6–7, $P < 0.05$).

Using 10 Hz frequency stimulation, but keeping the number of pulses unchanged, WIN55,212-2 alone elicited a clear concentration-dependent inhibitory effect on stimulation-evoked [^{3}H]NE release (Fig. 1E, G, F_{WIN} (1,66) = 6.461, P = 0.000061). The maximal effect of WIN55,212-2 was again obtained at 3 μM concentration, in which a 28.64 ± 6.93% inhibition was detected (n = 11). At this stimulation frequency, the interaction between WIN55,212-2 and idazoxan (1 μM) was also significant (Fig. 1G, $F_{interaction}$ (1,66) = 3.351, P = 0.0092). Interestingly, parallel relief from α_{2A}R-mediated autoinhibition by idazoxan occluded the effect of WIN55,212-2 at low concentration (0.3 μM), but exacerbated it at higher concentrations (3 and 10 μM, Fig. 1E–G): at this latter concentration the effect of WIN55,212-2 reached the level of significance in the presence of idazoxan only (Fig. 1G).

The inhibitory effect of WIN55,212-2 also exhibited frequency-dependence in the presence of idazoxan (1 μM): the maximal inhibition, obtained at the concentration of 3 μM, was significantly higher at 10 Hz (38.73 ± 2.07%, n = 6) than at 2 Hz (0.1 μM: 25.37 ± 2.59%, n = 7, $P < 0.01$). When calculated in absolute values, this treatment reduced NE efflux almost to the level of drug-free control (Fig. 1E, FRS2/FRS1 = 1.12 ± 0.04, n = 6).

The autoinhibition of [^{3}H]NE release by idazoxan (1 μM) was also well observable at 100 Hz stimulation frequency (Fig. 1H). Interestingly, however, WIN55,212-2, at the concentration (3 μM), which was effective at 2 and 10 Hz, did not change significantly the efflux of [^{3}H]NE at this high stimulation frequency, irrespectively from the absence or presence of idazoxan (Fig. 1H).

In order to examine whether the effect of WIN55,212-2 is mediated by CB_1Rs, the CB_1R-selective inverse agonist, AM251, was utilized. In absence of idazoxan, AM251 (1 μM) reversed the inhibitory effect of WIN55,212-2 on the evoked [^{3}H]NE efflux at 10 Hz (Fig. 2A). Likewise, in the combined presence of AM251 (1 μM) and idazoxan (1 μM), the inhibitory effect of WIN55,212-2 on the evoked [^{3}H]NE efflux was completely prevented (Fig. 2A). AM251, when applied alone in the absence of idazoxan, had no effect on basal (0.85 ± 0.05% and 1.00 ± 0.10% in the presence and absence of AM251, n = 6, $P > 0.05$) and stimulation-evoked [^{3}H]NE release (10 Hz: FRS2/FRS1 = 0.68 ± 0.04, n = 6, $P > 0.05$ vs. control). This result implies that, at least under drug-free conditions, CB_1Rs are not activated constitutively. By contrast, the anandamide reuptake inhibitor, VDM11 (10 μM), inhibited the evoked [^{3}H]NE efflux in the presence of idazoxan (1 μM) (Fig. 2A).

The previous experiments suggested that the efflux of [^{3}H]NE from the PFC is subject to an inhibitory neuromodulation by CB_1Rs and when autoinhibition by the α_{2A}Rs is relieved by idazoxan, a higher degree of inhibition can be detected at high concentrations of cannabinoid agonist at 10 Hz stimulation frequency (Fig. 1G). To further elucidate this interaction we next examined the effect of WIN55,212-2 (3 μM) in the presence of the α_{2A}Rs agonist xylazine (Fig. 2B). As expected, xylazine (0.01–3 μM) concentration-dependently decreased the stimulation-evoked efflux of [^{3}H]NE (Fig. 2C, $F_{xylazine}$ (1,61) = 2.187, P = 0.05), and at 3 μM concentration it attenuated the stimulation-evoked [^{3}H]NE efflux to a similar extent as WIN55,212-2 (3 μM) (Fig. 2B). Interestingly, the inhibitory action of WIN55,212-2 (3 μM) was occluded by xylazine at concentrations between 0.1 and 10 μM (Fig. 2B, C), i.e. their effects were not-additive.

Our data so far suggest that endogenously or exogenously activated α_{2A}Rs in the same presynaptic compartment occlude the inhibitory action CB_1Rs. Alternatively, the interaction between WIN55,212-2 and idazoxan is independent from α_{2A}Rs and is due to the increase of extracellular NE level evoked by idazoxan. To address this latter possibility we examined the effect of the psychostimulant drug amphetamine, which increases the extracellular level of NE, but is not a α_{2A}R ligand. As expected, amphetamine (30 μM) increased both basal (1.55 ± 0.08% and 1.06 ± 0.02%, n = 8, $P < 0.001$ in the presence and absence of amphetamine) and stimulation-evoked [^{3}H]NE efflux (Fig. 2D). The increase of the evoked [^{3}H]NE efflux, detected in the presence of amphetamine was nearly identical to the increase of the evoked [^{3}H]NE efflux elicited by idazoxan (Fig. 2D, 94.27 ± 28.11% increase). When WIN55,212-2 (3 μM) was administered together with amphetamine, however, no significant inhibition of the tritium release was observed (Fig. 2D).

3.2. Behavior experiments

In order to find a potential behavioral readout of interaction between CB_1Rs and α_{2A}Rs, as revealed in the previous experiments,

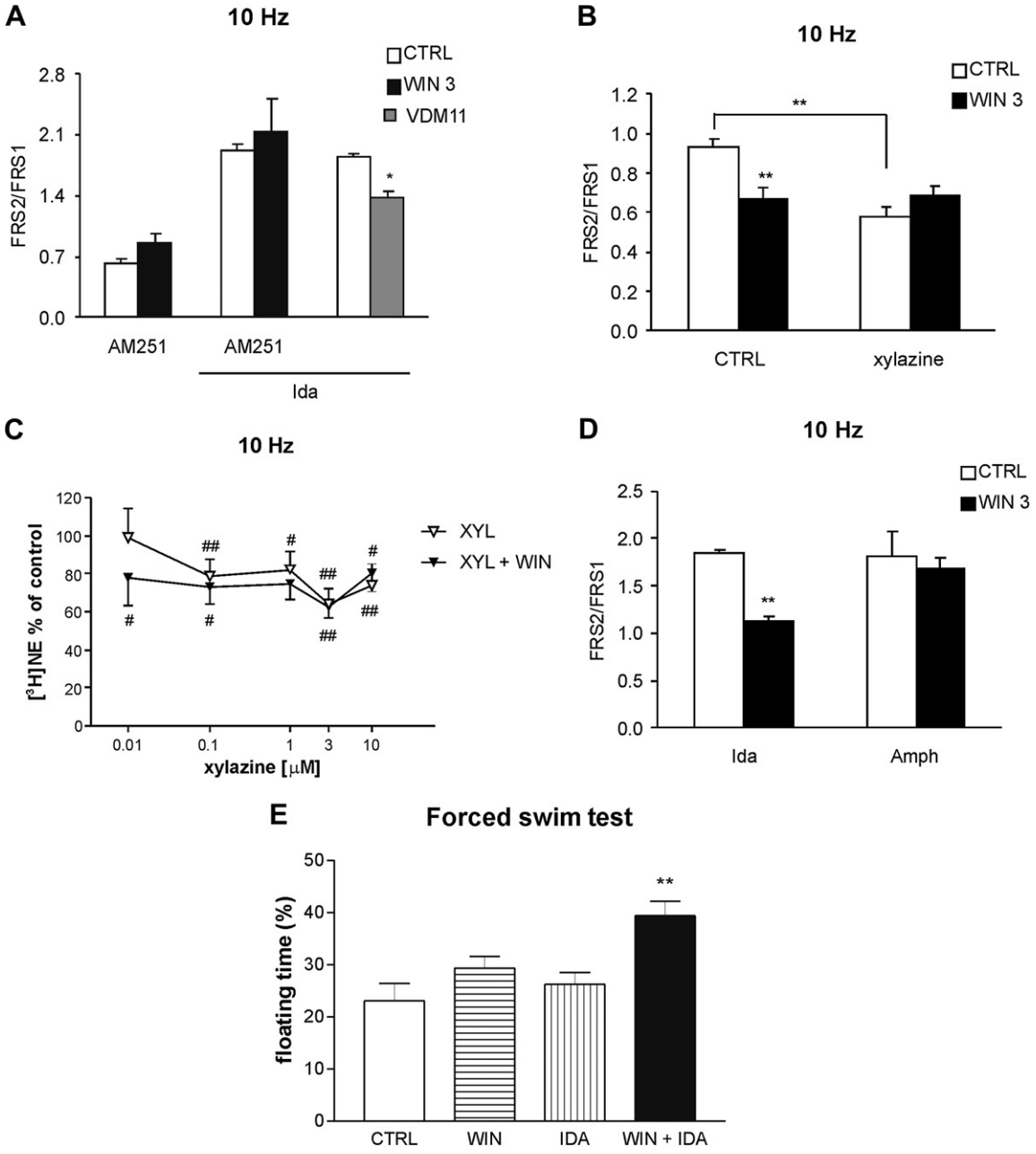

Fig. 2. A: Co-application of CB_1R inverse agonist AM251 (1 μM) reversed the inhibitory effect of WIN55,212-2 (3 μM, WIN 3) at 10 Hz stimulation highlighting the involvement of CB_1R receptors in the studied mechanism. Experiments were performed in the absence or presence of idazoxan, as indicated by the horizontal bar. Inhibition of anandamide reuptake by VDM11 (10 μM) decreased [^{3}H]NE release in the presence of idazoxan. Data are expressed as FRS2/FRS1 ratios. Asterisk indicates significant difference from respective control, calculated by the Student's *t* test ($^*P < 0.05$). B: Xylazine (3 μM) alone decreased the stimulation-evoked efflux of [^{3}H]NE to a similar extent as WIN55,212-2 (3 μM). Simultaneous challenge of CB_1R by WIN55,212-2 (3 μM, WIN 3) and $\alpha_{2A}R$ by xylazine did not reveal additive inhibition. Data are expressed as FRS2/FRS1 ratios. Asterisks indicate significant differences from respective control, or between CTRL and xylazine treated slices, calculated by the Student's *t* test ($^{**}P < 0.01$). C: At 10 Hz EFS, α_2-agonist challenge concentration-dependently attenuates [^{3}H]NE release. Results imply that between 0.1 and 3 μM concentrations, xylazine has no additive effect with WIN55,212-2 (3 μM), and the effect of WIN55,212-2 is occluded. Results are expressed as percentage of respective control FRS2/FRS1 ratios. 2-way-ANOVA and Fisher LSD post-hoc test were performed ($^{\#}P < 0.05$, $^{\#\#}P < 0.01$, significant differences from respective controls). D: Application of amphetamine (30 μM, Amph) markedly enhanced [^{3}H]NE release, similarly to idazoxan, as reflected by elevated FRS2/FRS1 ratios. Co-application of WIN55,212-2 (3 μM, WIN 3) revealed only minimal inhibition not reaching the level of significance. Data are expressed as FRS2/FRS1 ratios, measured in the absence (CTRL) and presence of WIN55,212-2 (WIN 3). Asterisks indicate significant differences from respective controls ($^{**}P < 0.01$, Student's *t* test). A–D: Data represent the mean ± S.E.M. of 4–8 identical experiments. E: Interaction between CB_1R and $\alpha_{2A}Rs$ in a conventional 6-min forced swim paradigm. Neither WIN55,212-2 (WIN) nor idazoxan (IDA) alone affected floating time. However, their combined application (WIN + IDA) resulted in a significant increase in the time of immobility, i.e. elicited a depressive-like behavior. WIN55,212-2 (0.2 mg/kg), idazoxan (0.5 mg/kg i.p.) or their combination were injected i.p. 30 min before test. Each group represents 8 identical experiments. Asterisks indicate significant differences from control group treated with vehicle (CTRL) ($^{**}P < 0.01$, one-way ANOVA, followed by the Tukey test).

we examined the interaction of the two drugs *in vivo* in a single 6-min forced swim paradigm, which is believed to reflect altered level of monoamine transmitters, i.e. NE and 5-HT (Cryan and Holmes, 2005). The time of immobility in control experiments in saline treated rats was 23.05 ± 3.37% ($n = 8$), whereas the time of swimming and struggling were 38.06 ± 6.29% and 34.58 ± 4.07% ($n = 8$), respectively. In our experiments, WIN55,212-2, which was applied in a dose that does not affect locomotion (0.2 mg/kg

i.p., Drews et al., 2005), alone was without effect on the time of immobility (Fig. 2E), swimming and struggling (data not shown). Likewise, idazoxan (0.5 mg/kg i.p.) was also without effect on either parameters (Fig. 2E). However, when the two drugs were injected together, the time of immobility was significantly increased (Fig. 2E).

The locomotor activity of rats, expressed as the total covered distance during the test period, treated with saline or WIN55,212-2 (0.2 mg/kg i.p.) + idazoxan (0.5 mg/kg i.p.) was not significantly different (6162 ± 778 cm, $n = 8$, and 7617 ± 1173 cm, $n = 8$, respectively, $P > 0.05$), indicating that the increased immobility in the forced swim test detected after this treatment was not due to an alteration in the basal locomotor activity.

3.3. Triple immunolabeling experiments with CB_1Rs, a_{2A}Rs and DβH antisera

CB_1R staining in the rat and mouse brain was similar to previous publications (Fig. 3B and F) (Bodor et al., 2005; Uchigashima et al., 2007; Ferreira et al., in press) without staining in the CB_1R knockout mouse (Fig. 3G). In the rostral part of the neocortex containing the frontal cortex, CB_1R staining exhibited a laminated orchestration both in mice and rats (Fig. 3B and F), in accordance with previous findings (Harkany et al., 2005). In fluorescence microscopy images at low (5×) resolution, the α_{2A}R antisera labeled cell bodies in the CB_1R-rich regions, i.e. in the layers II–III, Va and VI (Fig. 3C), in concert with a previous observation (Aoki et al., 1994). At this

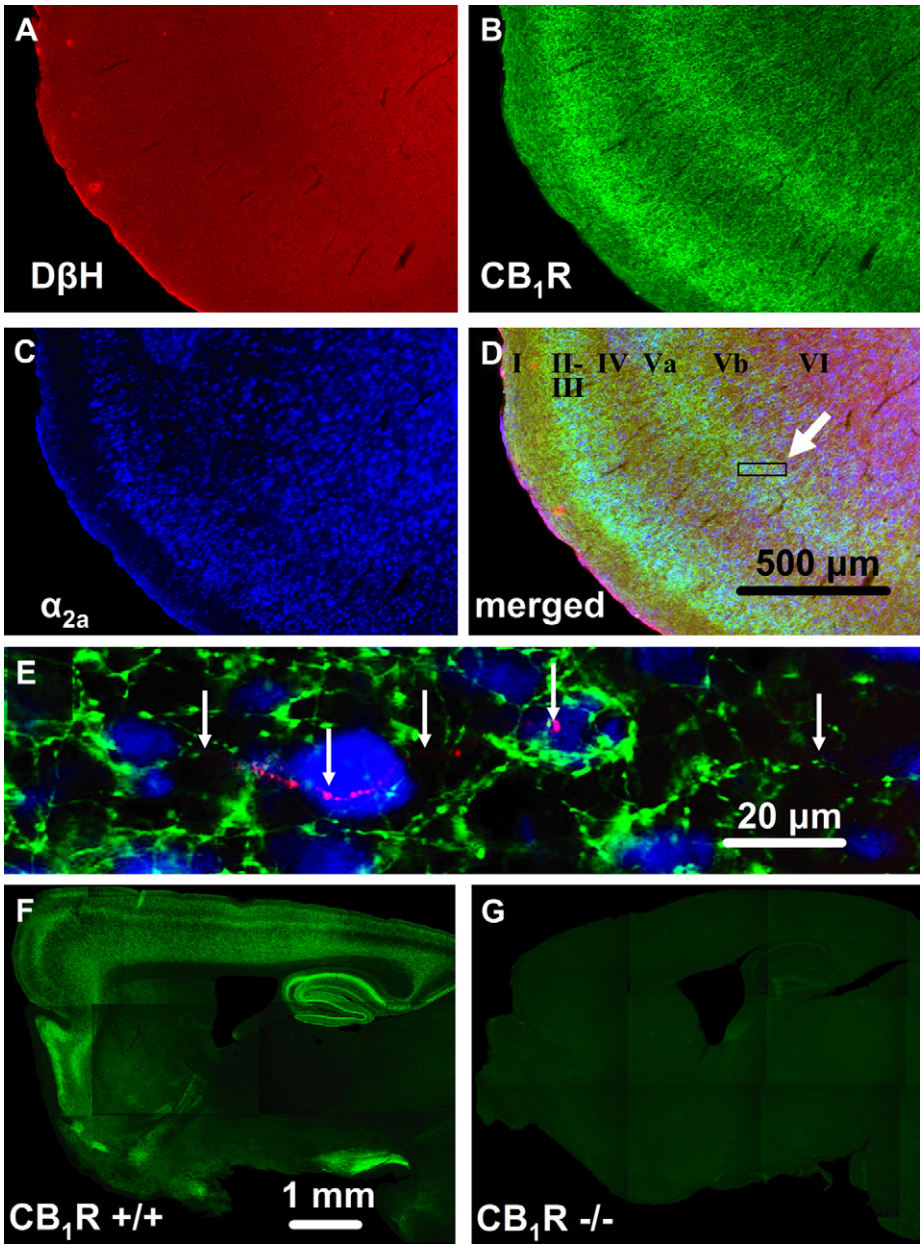

Fig. 3. Fluorescent microscopy images from sagittal slices of the rat and mouse brain. (A–D) Low magnification (5×) image showing the distribution of the dopamine-β-hydroxylase (DβH; red), CB_1 cannabinoid receptor (CB_1R; green) and α_{2A} adrenergic receptor (α_{2A}R; blue) immunoreactivity and their merged signal in a sagittal 30 µm-thick adult male Wistar rat brain slice. As panels B and F illustrate in the rat and mouse cortex, CB_1R staining is stronger in layers II–III, Va and VI. Note that in panel D, these layers are indicated with Roman numbers. Additionally in panel D, white arrow points toward the little rectangle excerpt from layer Va magnified at 40× in panel E. In panel E, a single noradrenergic terminal with lots of varicosities traverses the field as indicated by the vertical arrows. Between arrows 1 and 2 from the left, several varicosities appear to have immunostaining for CB_1R and α_{2A}R. Panels F and G illustrate the specificity of the CB_1R antisera under the conditions used in this study. The CB_1R null mutant (−/−) animal does not show structural staining with the CB_1R antibody.

resolution, DβH staining appeared homogenous, but at 40× magnification, many noradrenergic fibers were found to traverse the extracellular space (Fig. 3E). These fibers appeared strongly varicose, sometimes convoluted around each other, and many varicosities appeared to immunopositive for the CB_1R (in agreement with previous findings of Oropeza et al., 2007 and Reyes et al., 2009) or for $\alpha_{2A}R$ or both (Fig. 3E). To understand if these represent true or false co-localizations, we analyzed our slices further in confocal microscopy. At 63× magnification in optical slices in double immunostaining assay, DβH-positive fibers displayed discontinuous CB_1R immunoreactivity suggesting that CB_1Rs may localize primarily to the varicosities, i.e. close to the release sites (Fig. 4A1–3). The CB_1R-rich cortical layers displayed a highly dense meshwork of CB_1R-positive fibers, which are predominantly of

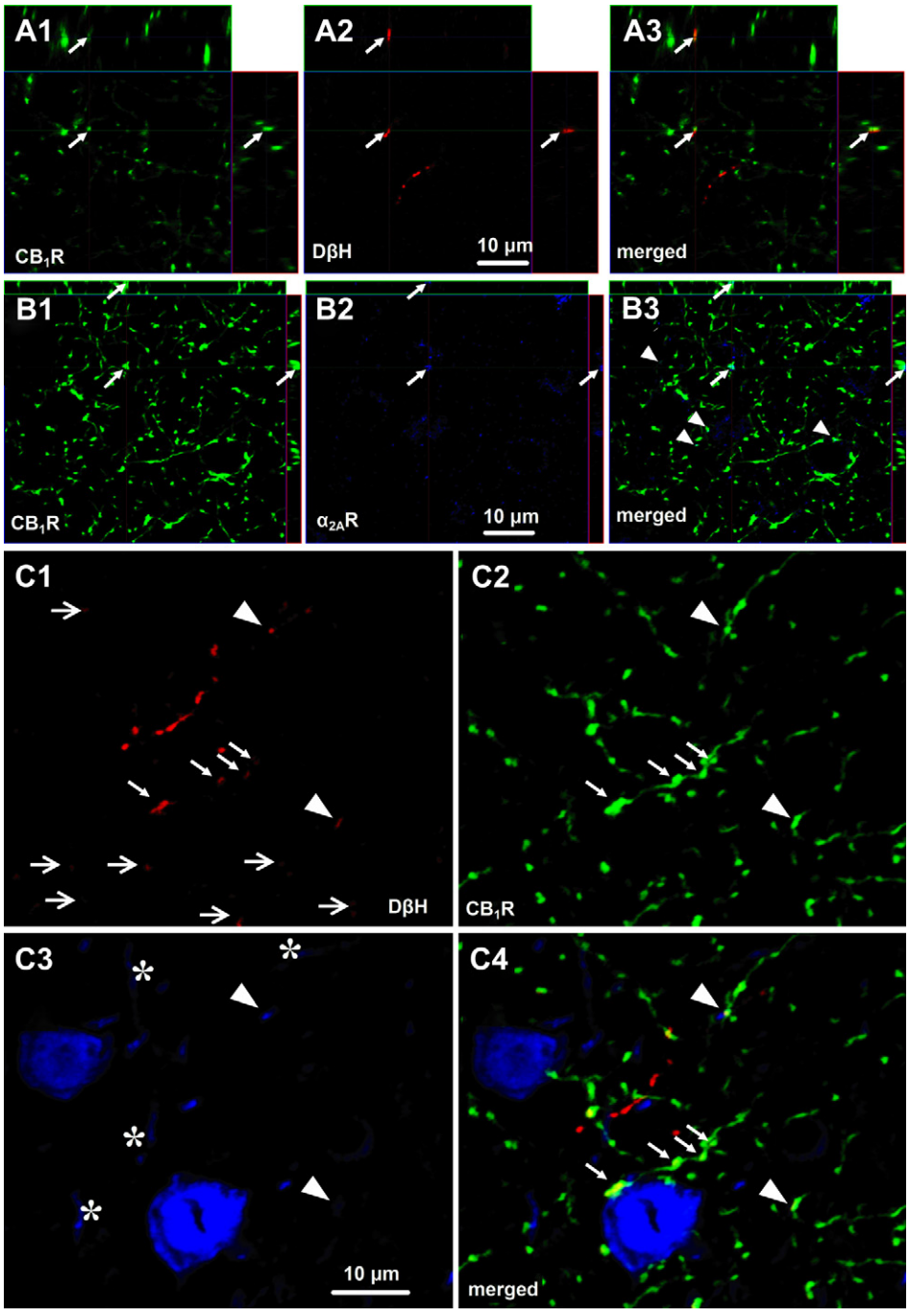

Fig. 4. CB_1R, DβH and $\alpha_{2A}R$ co-localization revealed by confocal microscopy in the rat frontal cortex. (A1–3) CB_1R (green; A1), DβH (red; A2) and merged signal (A3) in the layer VI of the frontal cortex of the rat. The yellow composite color is detected from all the three directions in the focus of the cross hair of the orthogonal projection of the 380 nm-thin optical section (marked with small arrows). (B1–3) CB_1R (green; B1), $\alpha_{2A}R$ (blue; B2) and merged signal (B3) in the layer II of the frontal cortex of the rat. Co-localization appears in turquoise from all the three directions in the focus of the cross hair, and is marked with small arrows. Full arrowheads point to other co-localizations in the same field (B3). (C1–4) Triple co-localization in the layer Va among DβH (red; C1) CB_1R (green; C2), and $\alpha_{2A}R$ (blue; C3). In panels (C1, 2, 4) the inclined small arrows point to CB_1R-positive varicosities of a DβH-positive fiber innervating an $\alpha_{2A}R$-positive cell. In this region, several other varicosities were detected with CB_1R staining (marked with horizontal, open arrows in C1). In panel (C3) asterisks label $\alpha_{2A}R$-positive, fiber-like structures. Throughout the four panels, full arrowheads point to sparsely appearing triple co-localizations. All images represent 380 nm-thin optical sections, photographed with a confocal microscope in a sagittal slice (63×/1.40 oil DIC M27, 1 × zoom, at 1024 dpi resolution).

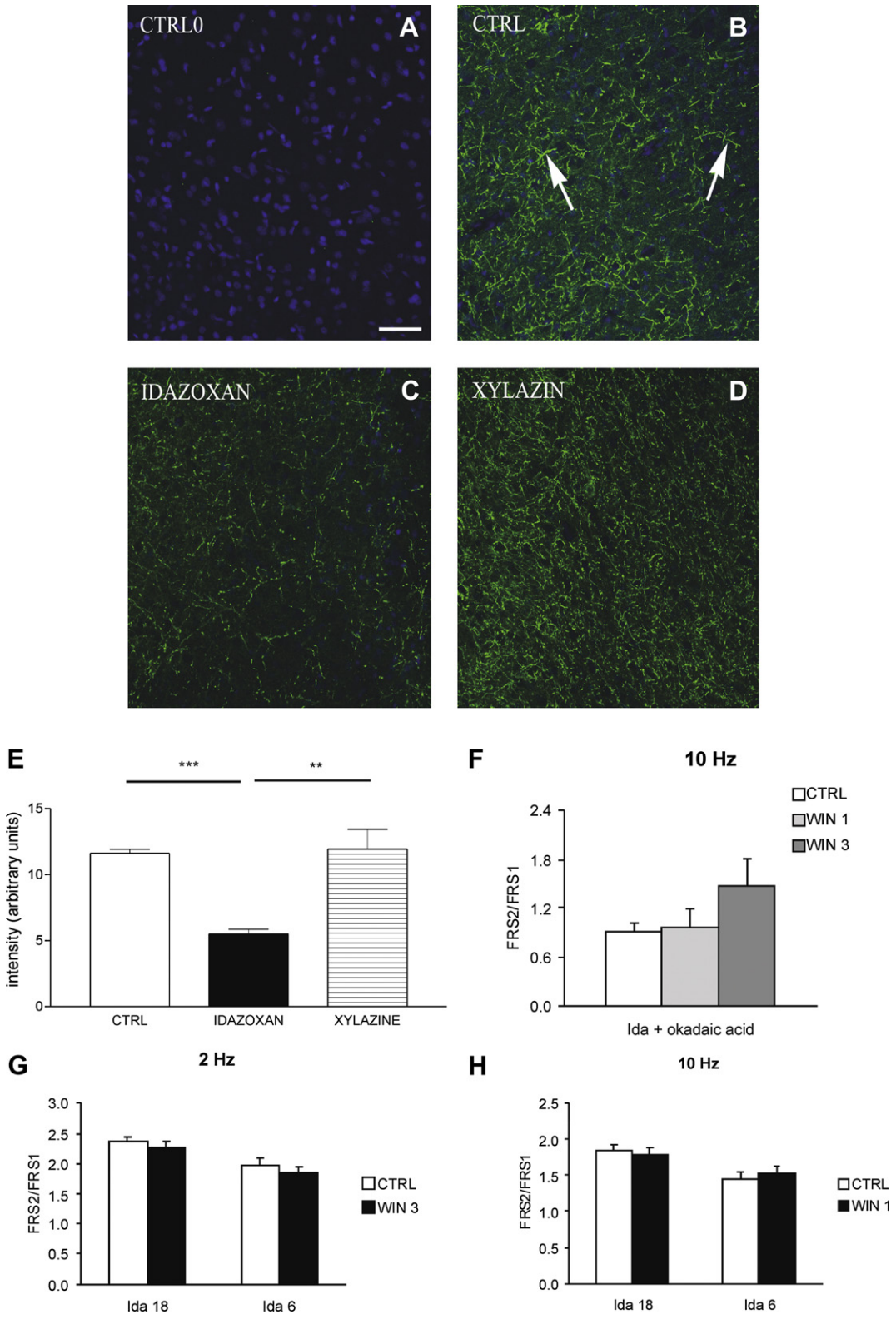

Fig. 5. Distribution of CB_1R in prefrontal cortex slice from Wistar rat after idazoxan (1 μM) and xylazine (3 μM) treatment. Immunofluorescence confocal micrographs were taken at the same area of prefrontal cortex containing layers 2–6 and at the same depth (10 μm) of the section. Green a-CB_1R-DyLight 488 conjugates label CB_1R immunopositive elements and DAPI stains nuclei. A: CTRL0: control of immunostaining. No green signal is visible when CB_1R antibody was omitted. B: CTRL: Strong immunoreactivity is presented in the axons as green lines (two of them labeled with arrows) and punctuated immunostaining in the boutons of the neurons in control cortical sections. C: After idazoxan treatment, altogether weaker green signal shows CB_1R immunopositivity. D: Apparently unchanged CB_1R immunoreactivity in axons and boutons was detected after xylazine treatment. Scale bar: 25 μm. E: Densitometric analyses of the data, performed by the ImageJ program. Statistical analyses were done by ANOVA + Tukey test. Asterisks indicate significant changes, $^{**}p < 0.01$, $n = 4$ in each group. F. The inhibitory effect of WIN55,212-2 (1–3 μM) on the stimulation-evoked efflux of [^{3}H]NE, measured in the presence of idazoxan (1 μM) is occluded by simultaneous application of the phosphatase inhibitor okadaic acid (80 nM). Data are expressed as FRS2/FRS1 ratios, measured in the absence (CTRL) and presence of WIN55,212-2. Data represent the mean ± S.E.M. of 4–8 identical experiments. G, H: Time-dependence of the attenuation of the effect of WIN55,212-2 on the stimulation-evoked

putative GABAergic and glutamatergic nature. Occasionally, some fibers appeared to be α_{2A}R-positive in double immunostaining (Fig. 4A1–3). In triple co-localization assay, intermittently CB_1R-, DβH- and α_{2A}R-positive fibers frequently surrounded α_{2A}R-positive cell bodies in the CB_1R-rich regions of the frontal cortex (Fig. 4C1–4). Thus, although the double co-localizations of CB_1R and DβH have already been reported in the frontal cortex, this is the first evidence indicating that the three markers may co-localize with each other in the same presynaptic compartment.

3.4. Agonist induced heterologous desensitization and subsequent internalization might play a role in the interaction between CB_1R and α_{2A}Rs

The above experiments clarified the mechanism underlying the occlusive interaction between the activation of α_{2A}R and of CB_1Rs. However, we have also observed an attenuation of the effect of WIN55,212-2 in the presence of idazoxan using 3 μM concentration at 2 Hz (Fig. 1F, G), and 0.3 μM at 10 Hz (Fig. 1G). Moreover, the presence of amphetamine (Fig. 2E) also abolished the effect of WIN55,212-2 (Fig. 2D), which suggested that elevated level of endogenous NE could also affect CB_1R-responsiveness, but in an opposite direction. Agonist induced heterologous desensitization and subsequent receptor internalization could be implicated in this phenomenon, as it is described for the interaction between other GPCRs (Cordeaux and Hill, 2002). In order to examine the putative changes of CB_1R protein density in response to the endogenous/exogenous activation of α_{2A}Rs, immunohistochemical staining was performed in microscopy sections from freshly prepared PFC slices, undergone idazoxan/xylazine treatments identical to the procedures used in release experiments (Fig. 5). As described above, typically strong labeling showed CB_1R immunoreactivity in the axons and boutons of the neurons in control cortical sections (Fig. 5A) and the staining pattern was similar to the picture obtained in previous work in the somatosensory cortex (e.g. Bodor et al., 2005). After idazoxan treatment the overall signal showing CB_1R immunopositive axons and boutons decreased (Fig. 5C, E). On the contrary, the CB_1R signal remained largely unchanged after xylazine treatment (Fig. 5D, E). At this resolution, changes in the ratio of stained elements – axons and boutons – were not observable. These data suggest that endogenous, but not exogenous activation of α_{2A}Rs influences the number of CB_1Rs appositioned to the plasma membrane. To further confirm this type of interaction we examined the effect of WIN55,212-2 (3 μM) in the absence and presence of okadaic acid, a phosphatase inhibitor with selectivity for protein phosphatase 1 and 2A (PP1 and PP2A), which interacts with the dephosphorylation step of a previously described CB_1R internalization cycle (Hsieh et al., 1999; van Koppen and Jakobs, 2004) (Fig. 5F). Okadaic acid (80 nM) completely prevented the inhibitory effect of WIN55,212-2 (1–3 μM) measured in the presence of idazoxan (1 μM). We also examined the time-dependence of the attenuation of the effect WIN55,212-2 by idazoxan at 2 Hz (Fig. 5G) and 10 Hz (Fig. 5H). Interestingly, we could observe the attenuation by idazoxan already at 6 min exposure time at both frequencies, indicating a rapid CB_1R internalization in response to idazoxan treatment.

4. Discussion

For the first time we show 1) the presence of functional presynaptic CB_1Rs in noradrenergic terminals of the rat prefrontal cortex, 2) and that the function of these CB_1Rs is controlled by presynaptic α_{2A}Rs in the same presynaptic compartment.

We found that WIN55,212-2, a cannabinoid receptor agonist, exhibited a concentration-dependent inhibitory effect on stimulation-evoked [^{3}H]NE efflux from PFC slices, using either low (2 Hz) or higher (10 Hz) frequency stimulation. This effect was sensitive to inhibition by the selective CB_1R inverse agonist AM251, indicating that it is mediated by CB_1Rs. Therefore, our results are consistent with the concept that the primary effect of the activation of presynaptic CB_1Rs is the inhibition of transmitter release, as well as confirming the plethora of previous data supporting this idea (e.g. Schlicker and Kathmann, 2001). Our results are also in agreement with previous investigations showing that the activation of CB_1Rs inhibits the release of NE from sympathetic nerves (Gobel et al., 2000; Ishac et al., 1996; Schultheiss et al., 2005), the rat hippocampus and guinea-pig cerebral cortex (Schlicker et al., 1997). On the other hand, using *in vivo* microdialysis Page et al. (2008) found that local application of WIN55,212-2 increases NE efflux from rat PFC. There are a multiplicity of differences between the conditions of *in vivo* and *in vitro* experiments. Among those, the most obvious is that although the microcircuits are retained in brain slices, input and output connections are eliminated and only local effects are detected, whereas under *in vivo* conditions the reciprocal innervations from the target areas, such as the *locus coeruleus*, are preserved. Therefore, it is reasonable to assume that in the experiments of Page et al. (2008), the effect of WIN55,212-2 was mediated by extracortical pathways, and this might overrule the local inhibitory modulation detected in our experiments. Moreover, the effective concentration of WIN55,212-2 used was much higher in their study than in ours, which also reinforces the above mentioned explanation.

Heteromeric interactions between metabotropic receptors are delicately regulated by optimal ligand concentrations, and thus concentration–response curves are frequently bell-shaped, and this holds true for CB_1Rs, which frequently participates in heterodimers (Navarro et al., 2010; Fuxe et al., 2012). In our experiments, WIN55,212-2 also produced bell-shaped concentration–response curve at 2 Hz stimulation. Notably, by increasing the stimulation frequency to 10 and 100 Hz the occupancy of α_{2A}Rs by extracellular NE is expected to increase as the rate of synaptic removal is constant. Thus, at 10 Hz, WIN55,212-2 elicited a higher degree of inhibition than at 2 Hz, but at even higher α_{2A}R occupancy, i.e. at 100 Hz, the effect of WIN55,212-2 was lost again, resembling to a bell-shaped concentration–response curve for α_{2A}R activation. Alternatively, the tone of endocannabinoids is already saturated at this high stimulation frequency and therefore administration of WIN55,212-2 did not lead to a significant additional inhibition under our experimental conditions. Neuronal network oscillations of different frequencies, including theta (6–10 Hz) and gamma (30–120 Hz) band activities, are implicated in many of higher order brain functions, such as sensory processing, attention and working memory (Fries, 2009; Jensen et al., 2007) and their disturbances are thought contribute to the pathophysiology of schizophrenia and other psychoses (Lee et al., 2003). Therefore, the frequency-dependent effect of the cannabinoid agonist on NE release might also have relevance under pathological conditions. Hajos et al. (2008) demonstrated that activation of CB_1Rs interferes with neuronal network oscillations and impairs sensory gating in the limbic circuitry. In their study, activation of CB_1Rs lead to an initial increase and later attenuation of both theta and gamma power recorded over the medial PFC. Our results imply that theta and

efflux of [^{3}H]NE by idazoxan (Ida, 1 μM) at 2 Hz (G) and 10 Hz (H). Idazoxan was applied 18 and 6 min before the second stimulation period (EFS2) as indicated, whereas WIN55,212-2 was administered 18 min before EFS2 in the concentration indicated in the legend. Otherwise, the experiments were performed according to the protocol shown on Fig. 1A. Data represent the mean ± S.E.M. of 6–13 identical experiments.

gamma oscillations probably distinctly influence cannabinergic neuromodulation, the interplay between CB_1Rs and other neuromodulatory receptors and their participation in the disease process (Dzirasa et al., 2010).

In our experiments the maximal inhibitory effect of WIN55,212-2 varied between 25 and 38 %, depending on the experimental conditions. These data are again consistent with previous studies addressing cannabinergic modulation of other neurotransmitters (Schlicker and Kathmann, 2001) and with the immunohistochemical data of the present study showing that only a subpopulation of noradrenergic varicosities express CB_1R. These data and the detected interaction of cannabinergic modulation with α_{2A}R mediated autoinhibition strongly indicate that CB_1Rs, involved in the modulation of NE release, are expressed on prefrontal noradrenergic varicosities.

In immunohistochemical experiments we found that CB_1Rs stain mostly the layers II–III, IVa and VI of the frontal cortex in accordance with previous findings (Harkany et al., 2005; Ferreira et al., in press). The post-synaptic (cellular) localization of α_{2A}R immunostaining is overt from the layer II toward the bottom of the cortex except in layer IV, however, high resolution images revealed also pre-synaptic (or more correctly varicosity staining since most varicosities do not form synapses) in accordance with the known pre-synaptic autoreceptor role of the α_{2A}R. CB_1Rs co-localized with both DβH and α_{2A}Rs, supporting our view on the presynaptic nature of the interaction of the two receptors in noradrenergic terminals of the frontal cortex.

Interestingly, we observed two kind of interactions between CB_1R and α_{2A}R in our neurochemical experiments. The effect of the cannabinoid receptor agonist was exacerbated with simultaneous relief from α_{2A}R-mediated autoinhibition by idazoxan, when 10 Hz stimulation frequency was used at agonist concentration of 3 μM and higher (Fig. 1G). These findings corroborate preliminary data found in another study using guinea-pig hippocampus as a model system (Schlicker and Gothert, 1998). All these results show that autoinhibition of NE release occludes the cannabinoid mediated inhibitory modulation and either the CB_1R or the α_{2A}R activation can inhibit noradrenaline release, but their combined action does not reveal additive inhibition.

In contrast, the effect the cannabinoid receptor agonist was attenuated by idazoxan using 3 μM concentration at 2 Hz frequency (Fig. 1F) and 0.3 μM concentration at 10 Hz frequency (Fig. 1G).

There are several potential mechanisms for the interactions between α_{2A}Rs and CB_1Rs: (1) utilization of a common $G_{i/o}$ pool and subsequent signal transduction machinery (2) agonist-induced heterologous desensitization by internalization and non-functional receptor generation by phosphorylation, (3) hetero-dimeric interaction of α_{2A}Rs with CB_1Rs.

(1) Because both CB_1R and α_{2A}Rs are coupled to pertussis-sensitive $G_{i/o}$ proteins, a likely possibility is that they utilize a common $G_{i/o}$ pool and subsequent signal transduction machinery. Indeed, $G_{i/o}$ proteins are able to move freely between α_{2A}Rs and CB_1Rs and other G-protein coupled receptors in SCG neurons microinjected with the human CB_1R cDNA (Vasquez and Lewis, 1999). In our experiments, when both α_{2A}Rs and CB_1Rs were challenged with agonists, a non-additive effect of xylazine and WIN55,212-2 was observed, which also supports this possibility. Moreover, when the extracellular level of NE was elevated by amphetamine, no exacerbation of the effect of WIN55,212-2 was detected, which precludes the assumption that elevated NE, rather than a specific effect on α_{2A}Rs, is responsible for this interaction.

(2) In order to further elucidate the interaction between CB_1Rs and α_2-adrenoceptors we examined how CB_1R immunoreactivity is altered in prefrontal cortical slices after an identical idazoxan treatment to the one used in the release experiments. We observed that the overall intensity of CB_1R immunostaining decreased after idazoxan. The idazoxan-induced down-regulation of CB_1Rs was also manifested in release experiments, as the effect of WIN55,212-2 declined above 1 μM concentration in the presence of idazoxan, when 2 Hz frequency was used (see Fig. 1F). Cumulating evidence from transfection experiments on cell lines suggests a major role of the C-terminus of the CB_1R in heterologous desensitization and G-protein uncoupling (Daigle et al., 2008a,b; Ellis et al., 2006; Stadel et al., 2011). Furthermore, Ellis et al. (2006) suggest a novel pharmacological paradigm, whereby ligands modulate the function of receptors for which they have no significant inherent affinity by acting as regulators of receptor heterodimers. Our results indicate diverse peak inhibitory effects of WIN55,212-2 depending on stimulation frequency or the presence of idazoxan. Disruption of the autoinhibitory loop mediated by α_{2A}Rs leads to increased NE release from PFC slices. The endogenous agonist may then occupy and act on free α_{2A}Rs to activate G-protein-coupled receptor kinase family type of proteins (GRKs). Subsequent phosphorylation of specific serine and threonine residues in the carboxy-terminus of the CB_1R could lead to subsequent recruitment of β-arrestin and internalization of the CB_1R or uncoupling of G-protein sequestration. Studies on cell cultures suggest rapid CB_1 internalization mechanisms of reversible nature even following brief agonist exposure in the range of minutes (Hsieh et al., 1999). At this point receptor internalization can be reversed by a dephosphorylation step that is sensitive to the phosphatase inhibitor okadaic acid (Hsieh et al., 1999). Supporting this assumption, when the recycling of CB_1 receptors was occluded by okadaic acid, we could not observe any inhibitory effect on [^{3}H]NE efflux by WIN55,212-2. Therefore, our results strongly suggest that in addition to the utilization of a common $G_{i/o}$ pool and subsequent signal transduction machinery, agonist-induced heterologous desensitization by receptor internalization and non-functional receptor generation by phosphorylation also operate in the rat PFC. Such a sensitive coupling of CB_1R internalization and recycling may contribute to fine-tuning of NE release in this region. Activation of CB_1Rs has been reported to downregulate α_{2A}Rs in the nucleus accumbens (Carvalho et al., 2010), but not in the PFC (Reyes et al., 2009). By contrast, to our knowledge this is the first report on the reverse interaction, i.e. on the down-regulation of CB_1Rs by the ongoing activation of α_{2A}Rs. Our findings raise the assumption that disease- or drug-altered noradrenergic transmission in this brain region may also derange the endocannabinoid system and its neuromodulatory actions present in the PFC. However, because we could not reproduce the same effect with exogenous agonist (xylazine) application, it appears that this mechanism only operates, when the level of endogenous NE is influenced.

(3) The concept of hetero-dimerization of GPCRs has gained increasing experimental support (Milligan, 2009) and hetero-oligomeric interactions of cannabinoid receptors have been previously described for GPCRs other than α_{2A}Rs (Cordeaux and Hill, 2002; Mackie, 2005; Fuxe et al., 2012). Such interaction allows reciprocal modulation of receptor function, trafficking and/or ligand pharmacology. Therefore, this phenomenon may underlie the frequency-dependence seen in our experiments: at different stimulation frequencies the rate of extracellular NE accumulation, and hence, α_{2A}R occupation will differ, resulting in dissimilar concentration–response curves for the CB_1R agonist.

As a potential readout of the interaction between CB_1R and α_2-adrenergic receptors, we examined the behavior of the rats in a conventional 6-min forced swim paradigm. This behavioral model has previously been shown to be linked to the activity of LC noradrenergic neurons and their projections to the PFC, and it is assumed that drugs which elevate extracellular level of NE decrease immobility, while the opposite is expected from drugs decreasing extracellular NE level (Cryan and Holmes, 2005; Cryan et al., 2002). Interestingly, we found that alone neither WIN55,212-2 nor idazoxan affected floating time. However, their combined application resulted in a significant increase in the time of immobility, i.e. they precipitated a depressive-like behavior, indicating that the overall result of this interaction might be a decrease in the extracellular level of NE. Therefore, a plausible explanation for the appearance of this behavior is the exacerbation of the inhibitory effect of WIN55,212-2 on NE release by idazoxan. Nevertheless, because the majority of α_{2A}Rs in the PFC are postsynaptic, we cannot exclude their role in this interaction. Further, the involvement of other limbic regions known to participate in mood related behavioral changes should also be considered. Whilst our results are in line with a previous study using the same dose of idazoxan and showing no effect alone in forced swim test (Zhang et al., 2009), they are somewhat unexpected in that WIN55,212-2 alone did not elicit antidepressant effect in the FST in our hands, as seen in a previous study (Bambico et al., 2007) and in case of other cannabinoid agonists (Hill and Gorzalka, 2005; Jiang et al., 2005; Rutkowska and Jachimczuk, 2004). However, the effects of cannabinoids on behavior are complex and highly context-dependent (Haller et al., 2009; Viveros et al., 2005) and even subtle differences in experimental conditions may lead to different results. For instance, in our experiments, unlike from that of Bambico et al., a single 6 min test period was applied instead of the traditional two-day paradigm, which may provide some explanation for the discrepancy. Moreover, CB_1R-receptor antagonists also convey antidepressant effect in animal tests (Griebel et al., 2005; Shearman et al., 2003; Takahashi et al., 2008) and there are data supporting the association between cannabis use and later incidence of depression (Degenhardt et al., 2001). This suggests that the relationship between CB_1R activation and mood regulation is not unidirectional.

Although we exemplified the impact of the interaction between prefrontal CB_1Rs and α_{2A}Rs with the increased immobility forced swim test, this effect might not be the only behavioral consequence of interplay between these two receptors. α_{2A}Rs antagonists including idazoxan are in clinical development for various psychiatric indications such as schizophrenia and ADHD (Conn and Roth, 2008). Therefore our findings highlight the possibility that a prior or concurrent cannabis abuse might modify their action.

The inverse agonist of CB_1Rs, AM251, *per se* did not have an effect on basal and stimulation-evoked [^{3}H]NE release at high frequency stimulation whereas the anandamide reuptake inhibitor VDM11 slightly inhibited the evoked [^{3}H]NE efflux in the presence of idazoxan. These findings indicate that although under basal conditions endocannabinoids have a minor influence on NE release in the *in vitro* rat PFC endocannabinoid mediated inhibition is probably also unmasked by the simultaneous inhibition of α_{2A}Rs.

5. Conclusions

Dysfunction of the prefrontal cortex leads to abnormal neurotransmitter outputs to other limbic areas including the amygdala, hippocampus and nucleus accumbens. This explains a key role of this brain region in the pathophysiology of psychiatric disorders and their associated symptoms. The results of our experiments highlight a diverse interaction of the endocannabinoid system with noradrenergic signaling in this area. Notably, CB_1R activation inhibits norepinephrine release and this modulation is dependent on stimulation frequency as well as on the autoinhibition of α_{2A}Rs. Utilization of common signal transduction pathways as well as heterologous desensitization of the CB_1R by means of a phosphorylation-dependent internalization likely play a role in this interaction. Such a mechanism could contribute to the impairment of prefrontocortical functions by cannabinoids.

Funding

This work was supported by grants of the Hungarian Research and Development Fund (NN79957 to B.S.); the Hungarian Medical Research Council (ETT 05-102 to B.S.); the European Research Council ("294313-SERRACO" to B.S.) and Fundação para a Ciência e a Tecnologia of the Portuguese Government (PTDC/SAU-OSM/105663/2008 to A.K. and SFRH/BD/33467/2008 to S.G.F.).

Acknowledgments

The authors wish to thank Mr. László Barna, the Nikon Microscopy Center at IEM, Nikon Austria GmbH and Auro-Science Consulting Ltd for kindly providing microscopy support. The authors are grateful to Ms. Flóra Gölöncsér, who performed behavior tests, to Ms. Zsuzsanna Körössy, Ms. Anna Palotás and Ms. Beáta Méhész who contributed to [^{3}H]NE release experiments, to Mr. Rómeó Andó for his help in statistical analyses and to Prof. László Hunyady for helpful discussions. We are also grateful to Ms. Sonya Costa and Ms. Luísa Cortes for excellent help.

References

Aoki, C., Go, C.G., Venkatesan, C., Kurose, H., 1994. Perikaryal and synaptic localization of alpha 2A-adrenergic receptor-like immunoreactivity. Brain Res. 650, 181–204.

Aoki, C., Venkatesan, C., Go, C.G., Forman, R., Kurose, H., 1998. Cellular and subcellular sites for noradrenergic action in the monkey dorsolateral prefrontal cortex as revealed by the immunocytochemical localization of noradrenergic receptors and axons. Cereb. Cortex 8, 269–277.

Arnsten, A.F., Cai, J.X., Goldman-Rakic, P.S., 1988. The alpha-2 adrenergic agonist guanfacine improves memory in aged monkeys without sedative or hypotensive side effects: evidence for alpha-2 receptor subtypes. J. Neurosci. 8, 4287–4298.

Arnsten, A.F., 2011. Catecholamine influences on dorsolateral prefrontal cortical networks. Biol. Psychiatry 69 (12), e89–99.

Bambico, F.R., Katz, N., Debonnel, G., Gobbi, G., 2007. Cannabinoids elicit antidepressant-like behavior and activate serotonergic neurons through the medial prefrontal cortex. J. Neurosci. 27, 11700–11711.

Bodor, A.L., Katona, I., Nyiri, G., Mackie, K., Ledent, C., Hajos, N., Freund, T.F., 2005. Endocannabinoid signaling in rat somatosensory cortex: laminar differences and involvement of specific interneuron types. J. Neurosci. 25, 6845–6856.

Bossong, M.G., Niesink, R.J., 2010. Adolescent brain maturation, the endogenous cannabinoid system and the neurobiology of cannabis-induced schizophrenia. Prog. Neurobiol. 92 (3), 370–385.

Bymaster, F.P., Katner, J.S., Nelson, D.L., Hemrick-Luecke, S.K., Threlkeld, P.G., Heiligenstein, J.H., Morin, S.M., Gehlert, D.R., Perry, K.W., 2002a. Atomoxetine increases extracellular levels of norepinephrine and dopamine in prefrontal cortex of rat: a potential mechanism for efficacy in attention deficit/hyperactivity disorder. Neuropsychopharmacology 27, 699–711.

Bymaster, F.P., Zhang, W., Carter, P.A., Shaw, J., Chernet, E., Phebus, L., Wong, D.T., Perry, K.W., 2002b. Fluoxetine, but not other selective serotonin uptake inhibitors, increases norepinephrine and dopamine extracellular levels in prefrontal cortex. Psychopharmacology (Berl) 160, 353–361.

Canas, P.M., Duarte, J.M., Rodrigues, R.J., Köfalvi, A., Cunha, R.A., 2009. Modification upon aging of the density of presynaptic modulation systems in the hippocampus. Neurobiol. Aging 30, 1877–1884.

Carvalho, A.F., Mackie, K., Van Bockstaele, E.J., 2010. Cannabinoid modulation of limbic forebrain noradrenergic circuitry. Eur. J. Neurosci. 31, 286–301.

Conn, P.J., Roth, B.L., 2008. Opportunities and challenges of psychiatric drug discovery: roles for scientists in academic, industry, and government settings. Neuropsychopharmacology 33, 2048–2060.

Cordeaux, Y., Hill, S.J., 2002. Mechanisms of cross-talk between G-protein-coupled receptors. Neurosignals 11, 45–57.

Cryan, J.F., Holmes, A., 2005. The ascent of mouse: advances in modelling human depression and anxiety. Nat. Rev. Drug Discov. 4, 775–790.

Cryan, J.F., Markou, A., Lucki, I., 2002. Assessing antidepressant activity in rodents: recent developments and future needs. Trends Pharmacol. Sci. 23, 238–245.
Csölle, C., Heinrich, A., Kittel, A., Sperlagh, B., 2008. P2Y receptor mediated inhibitory modulation of noradrenaline release in response to electrical field stimulation and ischemic conditions in superfused rat hippocampus slices. J. Neurochem. 106, 347–360.
Daigle, T.L., Kearn, C.S., Mackie, K., 2008a. Rapid CB_1 cannabinoid receptor desensitization defines the time course of ERK1/2 MAP kinase signaling. Neuropharmacology 54, 36–44.
Daigle, T.L., Kwok, M.L., Mackie, K., 2008b. Regulation of CB_1 cannabinoid receptor internalization by a promiscuous phosphorylation-dependent mechanism. J. Neurochem. 106, 70–82.
Degenhardt, L., Hall, W., Lynskey, M., 2001. The relationship between cannabis use, depression and anxiety among Australian adults: findings from the National Survey of Mental Health and Well-Being. Soc. Psychiatry Psychiatr. Epidemiol. 36, 219–227.
Drews, E., Schneider, M., Koch, M., 2005. Effects of the cannabinoid receptor agonist WIN 55,212-2 on operant behavior and locomotor activity in rats. Pharmacol. Biochem. Behav. 80, 145–150.
Dzirasa, K., Phillips, H.W., Sotnikova, T.D., Salahpour, A., Kumar, S., Gainetdinov, R.R., Caron, M.G., Nicolelis, M.A., 2010 May 5. Noradrenergic control of cortico-striato-thalamic and mesolimbic cross-structural synchrony. J. Neurosci. 30 (18), 6387–6397.
Ellis, J., Pediani, J.D., Canals, M., Milasta, S., Milligan, G., 2006. Orexin-1 receptor-cannabinoid CB_1 receptor heterodimerization results in both ligand-dependent and -independent coordinated alterations of receptor localization and function. J. Biol. Chem. 281, 38812–38824.
Ferreira, S.G., Teixeira, F., Garção, P., Agostinho, P., Ledent, C., Cortes, L., Mackie, K., Köfalvi, A., Presynaptic CB_1 cannabinoid receptors control frontocortical serotonin and glutamate release – species differences. Neurochem. Int., in press.
Fries, P., 2009. Neuronal gamma-band synchronization as a fundamental process in cortical computation. Annu. Rev. Neurosci. 32, 209–224.
Fukudome, Y., Ohno-Shosaku, T., Matsui, M., Omori, Y., Fukaya, M., Tsubokawa, H., Taketo, M.M., Watanabe, M., Manabe, T., Kano, M., 2004. Two distinct classes of muscarinic action on hippocampal inhibitory synapses: M2-mediated direct suppression and M1/M3-mediated indirect suppression through endocannabinoid signalling. Eur. J. Neurosci. 19, 2682–2692.
Fuxe, K., Borroto-Escuela, D.O., Marcellino, D., Romero-Fernandez, W., Frankowska, M., Guidolin, D., Filip, M., Ferraro, L., Woods, A.S., Tarakanov, A., Ciruela, F., Agnati, L.F., Tanganelli, S., 2012. GPCR heteromers and their allosteric receptor-receptor interactions. Curr. Med. Chem. 19, 356–363.
Gamo, N.J., Arnsten, A.F., 2011. Molecular modulation of prefrontal cortex: rational development of treatments for psychiatric disorders. Behav. Neurosci. 125 (3), 282–296.
Gobel, I., Trendelenburg, A.U., Cox, S.L., Meyer, A., Starke, K., 2000. Electrically evoked release of [(3)H]noradrenaline from mouse cultured sympathetic neurons: release-modulating heteroreceptors. J. Neurochem. 75, 2087–2094.
Griebel, G., Stemmelin, J., Scatton, B., 2005. Effects of the cannabinoid CB_1 receptor antagonist rimonabant in models of emotional reactivity in rodents. Biol. Psychiatry 57, 261–267.
Hajós, M., Hoffmann, W.E., Kocsis, B., 2008. Activation of cannabinoid-1 receptors disrupts sensory gating and neuronal oscillation: relevance to schizophrenia. Biol. Psychiatry 63, 1075–1083.
Haller, J., Barna, I., Barsvari, B., Gyimesi Pelczer, K., Yasar, S., Panlilio, L.V., Goldberg, S., 2009. Interactions between environmental aversiveness and the anxiolytic effects of enhanced cannabinoid signaling by FAAH inhibition in rats. Psychopharmacology (Berl) 204, 607–616.
Harkany, T., Dobszay, M.B., Cayetanot, F., Härtig, W., Siegemund, T., Aujard, F., Mackie, K., 2005. Redistribution of CB_1 cannabinoid receptors during evolution of cholinergic basal forebrain territories and their cortical projection areas: a comparison between the gray mouse lemur (*Microcebus murinus*, primates) and rat. Neuroscience 135, 595–609.
Hill, M.N., Gorzalka, B.B., 2005. Pharmacological enhancement of cannabinoid CB_1 receptor activity elicits an antidepressant-like response in the rat forced swim test. Eur. Neuropsychopharmacol. 15, 593–599.
Hsieh, C., Brown, S., Derleth, C., Mackie, K., 1999. Internalization and recycling of the CB_1 cannabinoid receptor. J. Neurochem. 73 (2), 493–501.
Ishac, E.J., Jiang, L., Lake, K.D., Varga, K., Abood, M.E., Kunos, G., 1996. Inhibition of exocytotic noradrenaline release by presynaptic cannabinoid CB_1 receptors on peripheral sympathetic nerves. Br. J. Pharmacol. 118, 2023–2028.
Jensen, O., Kaiser, J., Lachaux, J.P., 2007. Human gamma-frequency oscillations associated with attention and memory. Trends Neurosci. 30, 317–324.
Jiang, W., Zhang, Y., Xiao, L., Van Cleemput, J., Ji, S.P., Bai, G., Zhang, X., 2005. Cannabinoids promote embryonic and adult hippocampus neurogenesis and produce anxiolytic- and antidepressant-like effects. J. Clin. Invest. 115, 3104–3116.
Kathmann, M., Bauer, U., Schlicker, E., Gothert, M., 1999. Cannabinoid CB_1 receptor-mediated inhibition of NMDA- and kainate-stimulated noradrenaline and dopamine release in the brain. Naunyn Schmiedebergs Arch. Pharmacol. 359, 466–470.
Koob, G., Kreek, M.J., 2007. Stress, dysregulation of drug reward pathways, and the transition to drug dependence. Am. J. Psychiatry 164 (8), 1149–1159.
Koob, G.F., Volkow, N.D., 2010. Neurocircuitry of addiction. Neuropsychopharmacology 35, 217–238.
Lafourcade, M., Elezgarai, I., Mato, S., Bakiri, Y., Grandes, P., Manzoni, O.J., 2007. Molecular components and functions of the endocannabinoid system in mouse prefrontal cortex. PLoS One 2, e709.
Ledent, C., Valverde, O., Cossu, G., Petitet, F., Aubert, J.F., Beslot, F., Bohme, G.A., Imperato, A., Pedrazzini, T., Roques, B.P., Vassart, G., Fratta, W., Parmentier, M., 1999. Unresponsiveness to cannabinoids and reduced addictive effects of opiates in CB_1 receptor knockout mice. Science 283, 401–404.
Lee, K.H., Williams, L.M., Breakspear, M., Gordon, E., 2003. Synchronous gamma activity: a review and contribution to an integrative neuroscience model of schizophrenia. Brain Res. Brain Res. Rev. 41, 57–78.
Mackie, K., 2005. Cannabinoid receptor homo- and heterodimerization. Life Sci. 77, 1667–1673.
Malone, D.T., Hill, M.N., Rubino, T., 2010. Adolescent cannabis use and psychosis: epidemiology and neurodevelopmental models. Br. J. Pharmacol. 160 (3), 511–522.
Milligan, G., 2009. G protein-coupled receptor hetero-dimerization: contribution to pharmacology and function. Br. J. Pharmacol. 158, 5–14.
Navarro, G., Ferré, S., Cordomi, A., Moreno, E., Mallol, J., Casadó, V., Cortés, A., Hoffmann, H., Ortiz, J., Canela, E.I., Lluís, C., Pardo, L., Franco, R., Woods, A.S., 2010. Interactions between intracellular domains as key determinants of the quaternary structure and function of receptor heteromers. J. Biol. Chem. 285, 27346–27359.
Nissen, S.E., Nicholls, S.J., Wolski, K., Rodes-Cabau, J., Cannon, C.P., Deanfield, J.E., Despres, J.P., Kastelein, J.J., Steinhubl, S.R., Kapadia, S., Yasin, M., Ruzyllo, W., Gaudin, C., Job, B., Hu, B., Bhatt, D.L., Lincoff, A.M., Tuzcu, E.M., 2008. Effect of rimonabant on progression of atherosclerosis in patients with abdominal obesity and coronary artery disease: the STRADIVARIUS randomized controlled trial. JAMA 299, 1547–1560.
Oropeza, V.C., Mackie, K., Van Bockstaele, E.J., 2007. Cannabinoid receptors are localized to noradrenergic axon terminals in the rat frontal cortex. Brain Res. 1127, 36–44.
Oropeza, V.C., Page, M.E., Van Bockstaele, E.J., 2005. Systemic administration of WIN 55,212-2 increases norepinephrine release in the rat frontal cortex. Brain Res. 1046, 45–54.
Page, M.E., Oropeza, V.C., Van Bockstaele, E.J., 2008. Local administration of a cannabinoid agonist alters norepinephrine efflux in the rat frontal cortex. Neurosci. Lett. 431, 1–5.
Paxinos, G., Watson, C., 1998. The Rat Brain in Stereotaxic Coordinates, fourth Ed. Academic Press, New York.
Ramos, B., Arnsten, A., 2007. Adrenergic pharmacology and cognition: focus on the prefrontal cortex. Pharmacol. Ther. 113 (3), 523–536.
Reyes, B.A., Rosario, J.C., Piana, P.M., Van Bockstaele, E.J., 2009. Cannabinoid modulation of cortical adrenergic receptors and transporters. J. Neurosci. Res. 87, 3671–3678.
Rutkowska, M., Jachimczuk, O., 2004. Antidepressant–like properties of ACEA (arachidonyl-2-chloroethylamide), the selective agonist of CB_1 receptors. Acta Pol. Pharm. 61, 165–167.
Schlicker, E., Gothert, M., 1998. Interactions between the presynaptic alpha2-autoreceptor and presynaptic inhibitory heteroreceptors on noradrenergic neurones. Brain Res. Bull. 47, 129–132.
Schlicker, E., Kathmann, M., 2001. Modulation of transmitter release via presynaptic cannabinoid receptors. Trends Pharmacol. Sci. 22, 565–572.
Schlicker, E., Timm, J., Zentner, J., Gothert, M., 1997. Cannabinoid CB_1 receptor-mediated inhibition of noradrenaline release in the human and guinea-pig hippocampus. Naunyn Schmiedebergs Arch. Pharmacol. 356, 583–589.
Schultheiss, T., Flau, K., Kathmann, M., Gothert, M., Schlicker, E., 2005. Cannabinoid CB_1 receptor-mediated inhibition of noradrenaline release in guinea-pig vessels, but not in rat and mouse aorta. Naunyn Schmiedebergs Arch. Pharmacol. 372, 139–146.
Shearman, L.P., Rosko, K.M., Fleischer, R., Wang, J., Xu, S., Tong, X.S., Rocha, B.A., 2003. Antidepressant-like and anorectic effects of the cannabinoid CB_1 receptor inverse agonist AM251 in mice. Behav. Pharmacol. 14, 573–582.
Stadel, R., Ahn, K.H., Kendall, D.A., 2011. The cannabinoid type-1 receptor carboxyl-terminus, more than just a tail. J. Neurochem. 117, 1–18.
Starke, K., 2001. Presynaptic autoreceptors in the third decade: focus on alpha2-adrenoceptors. J. Neurochem. 78, 685–693.
Takahashi, E., Katayama, M., Niimi, K., Itakura, C., 2008. Additive subthreshold dose effects of cannabinoid CB(1) receptor antagonist and selective serotonin reuptake inhibitor in antidepressant behavioral tests. Eur. J. Pharmacol. 589, 149–156.
Tzavara, E.T., Davis, R.J., Perry, K.W., Li, X., Salhoff, C., Bymaster, F.P., Witkin, J.M., Nomikos, G.G., 2003. The CB_1 receptor antagonist SR141716A selectively increases monoaminergic neurotransmission in the medial prefrontal cortex: implications for therapeutic actions. Br. J. Pharmacol. 138, 544–553.
Uchigashima, M., Narushima, M., Fukaya, M., Katona, I., Kano, M., Watanabe, M., 2007. Subcellular arrangement of molecules for 2-arachidonoyl-glycerol-mediated retrograde signaling and its physiological contribution to synaptic modulation in the striatum. J. Neurosci. 27, 3663–3676.
van Koppen, C.J., Jakobs, K.H., 2004. Arrestin-independent internalization of G protein-coupled receptors. Mol. Pharmacol. 66, 365–367.
Vasquez, C., Lewis, D.L., 1999. The CB_1 cannabinoid receptor can sequester G-proteins, making them unavailable to couple to other receptors. J. Neurosci. 19, 9271–9280.
Viveros, M.P., Marco, E.M., File, S.E., 2005. Endocannabinoid system and stress and anxiety responses. Pharmacol. Biochem. Behav. 81, 331–342.

Wang, M., Ramos, B.P., Paspalas, C.D., Shu, Y., Simen, A., Duque, A., Vijayraghavan, S., Brennan, A., Dudley, A., Nou, E., Mazer, J.A., McCormick, D.A., Arnsten, A.F., 2007. Alpha2A-adrenoceptors strengthen working memory networks by inhibiting cAMP-HCN channel signaling in prefrontal cortex. Cell 129, 397–410.

Westerink, B.H., Kawahara, Y., De Boer, P., Geels, C., De Vries, J.B., Wikstrom, H.V., Van Kalkeren, A., Van Vliet, Kruse, C.G., Long, S.K., 2001. Antipsychotic drugs classified by their effects on the release of dopamine and noradrenaline in the prefrontal cortex and striatum. Eur. J. Pharmacol. 412, 127–138.

Zhang, H.T., Whisler, L.R., Huang, Y., Xiang, Y., O'Donnell, J.M., 2009. Post-synaptic alpha-2 adrenergic receptors are critical for the antidepressant-like effects of desipramine on behavior. Neuropsychopharmacology 34, 1067–1077.

Zhang, W., Perry, K.W., Wong, D.T., Potts, B.D., Bao, J., Tollefson, G.D., Bymaster, F.P., 2000. Synergistic effects of olanzapine and other antipsychotic agents in combination with fluoxetine on norepinephrine and dopamine release in rat prefrontal cortex. Neuropsychopharmacology 23, 250–262.